# Excited-state intramolecular proton transfer in the anionic species of 2-(2′-acetamidophenyl)benzimidazole in aqueous medium

**ARTICLE** *in* CHEMICAL PHYSICS LETTERS · SEPTEMBER 2000

Impact Factor: 1.9 · DOI: 10.1016/S0009-2614(00)00807-1



**3 AUTHORS**, INCLUDING:

Swadeshmukul Santra
University of Central Florida
**89** PUBLICATIONS **4,636** CITATIONS

SEE PROFILE

S. K. Dogra
Indian Institute of Technology Kanpur
**129** PUBLICATIONS **2,201** CITATIONS

SEE PROFILE

8 September 2000

ELSEVIER

Chemical Physics Letters 327 (2000) 230–237

CHEMICAL PHYSICS LETTERS

www.elsevier.nl/locate/cplett

# Excited-state intramolecular proton transfer in the anionic species of 2-(2′-acetamidophenyl) benzimidazole in aqueous medium

Swadeshmukul Santra, G. Krishnamoorthy, Sneh K. Dogra *

*Department of Chemistry, Indian Institute of Technology Kanpur, Kanpur 208 016, India*

Received 23 March 2000; in final form 20 June 2000

**Abstract**

An excited-state intramolecular proton transfer (ESIPT) process has been observed in the anionic species of 2-(2′-acetamidophenyl)benzimidazole (2-AMPBI). Dual fluorescence is observed in the case of monoanionic species. The presence of different monoanionic species has been characterized by means of steady-state and time-resolved fluorescene spectroscopy, as well as using AM1 semi-empirical quantum-mechanical calculations. The present study revealed that the presence of an acetyl group plays a vital role in the stability of different ionic and neutral species and in changes in their ground ($S_0$) and excited singlet state ($S_1$) acid–base properties with respect to 2-(2′-aminophenyl)benzimidazole (2-APBI).


## 1. Introduction

The process of excited-state intramolecular proton transfer (ESIPT) which typically shows a largely Stokes shifted fluorescence band has become a field of active research [1–7] due to its widespread implications as ultraviolet (UV) stabilization [8,9], stimulated radiation production [10,11], information storage [12], fluorescent solar concentrator [13], as well as environmental probes in biomolecules [14]. In organic bifunctional molecules which contain both hydrogen-atom donor (e.g., –OH, $-NH_2$, etc.) and acceptor (=N–, >C=O, etc.) groups in close proximity, an intramolecular hydrogen bond (IBH) is generally formed in the ground state. The intramolecular redistribution of electronic charge due to photonic excitation induces the ESIPT process which is ultrafast in nature ($k_{ESIPT} > 10^{12}$ $s^{-1}$) and is complete in less than 8 ps at room temperature [15]. A large rate constant is presumably due to the fact that the process involves very slight ($\sim 1$ Å) movement of a light hydrogen atom.

For the past two decades, our laboratory has largely been involved in synthesizing new molecular systems showing ESIPT and in studying their photophysical properties [16–19]. Recently the 2-AMPBI molecule (Scheme 1) has been synthesized by the substitution of one of the amino hydrogen atoms of 2-APBI by the electron withdrawing acetyl group to increase polarizability of the remaining hydrogen atom. This increased the strength of IBH. As a result, the tautomer emission was nearly 12 times greater than that observed in 2-APBI in cyclohexane; in water, present molecule (2-AMPBI) contains two acidic protons (>N–H and amido). Deprotonation

* Corresponding author. Fax: +91-512-590007; e-mail: skdogra@iitk.ac.in

0009-2614/00/$ - see front matter 
PII: S0009-2614(00)00807-1

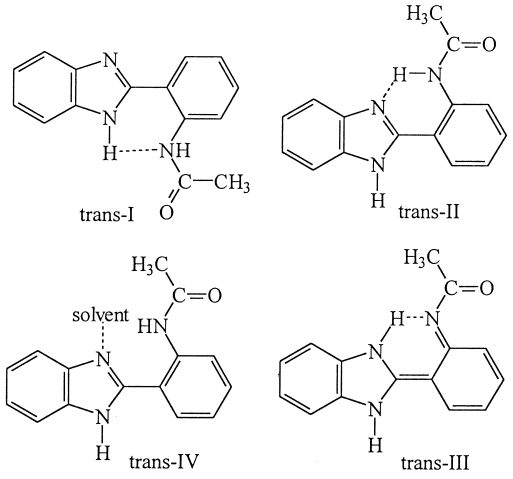


Scheme 1. Geometry of the different conformers of 2-AMPBI.

of even one of these can still lead to the formation of IBH between the two rings and thus lead to the ESIPT process. If this process does occur, to the best our knowledge, it will be the first example of ESIPT in anionic species.

## 2. Materials and methods

2-AMPBI was synthesized from 2-APBI and purified as suggested in the literature [20]. AnalR grade methanol (E. Merck) was further purified as described [21]. Triply distilled water was used for the preparation of aqueous solution. The pH of the solutions in the range of 3–11 was adjusted by adding an appropriate amount of *o*-phosphoric acid and NaOH. Yagil's basicity scale [22] for the $NaOH–H_2O$ mixtures was used for solutions above pH = 13.

The instruments used to record absorption, fluorescence and fluorescence excitation spectra, time-resolved spectrofluorimeter and the procedure used to measure fluorescence quantum yield are the same as described in our earlier paper [20]. The concentration of test solutions was $4 \times 10^{-5}$ M for lifetime measurements; for other experiments, the concentration was $2 \times 10^{-5}$ M in 2% methanol (v/v) in water. Solutions for absorptiometric and fluorometric titrations were prepared just before taking measurements. Isosbestic wavelengths were used to measure the relative fluorescence intensities at the analytical wavelengths to calculate the excited state $pK_a$ ($pK_a^*$) values for different prototropic reactions.

Two kinds of monoanions (MAs, MA-I and MA-III; formed by the deprotonation of amido proton and >N–H proton, respectively) and two rotamers of each MA and tautomer MA (MA-IV), as well as the solvated species MA-II and MA-IV′, are shown in Scheme 3. The ground-state geometries of all the species, except for the solvated ones, were optimized using the AM1 method (QCMP 137, MOPAC 6/PC) [23]. The total energy ($E_{iso}$) and dipole moment ($\mu_g$) are given in Scheme 3. The dipolar solvation energy in water for each species was calculated using the following relation [24]

$$\Delta E_{sol} = \left(-\mu^2/4\pi \in_0 a^3\right) f(\in)$$

where $f(\in) = (\in -1)/(2 \in +1)\mu$ is the dipole moment of the respective species in the respective state and $a$ is the Onsager's cavity radius. The total energy, including the solvation energy, for each species has also been complied in Scheme 3.

## 3. Results and discussion

Salient features of the spectral characteristics of neutral 2-AMPBI are given briefly in order to compare the results of the ionic species with those for the neutral 2-AMPBI which is neutral in the pH range of 6–10, having absorption band maximum at 293 nm with a long tail towards red with shoulder at ~330 nm (Scheme 2). Dual fluorescence is observed in all the solvents with a band maximum at 367 nm (normal emission) and 473 nm (tautomer emission) (Fig. 1, Scheme 2). Fluorescene, fluorescence excitation spectra, time-correlated emission studies, combined with semi-empiricial AM1 quantum-mechanical calculations, have shown that: (i) 2-AMPBI is present only as a *trans* form (both >N–H and >C=O groups are present on the opposite side; Scheme 1), (ii) three distinct species are present in the aqueous medium in the $S_0$ state (rotamer *trans*-I, rotamer *trans*-II and solvated rotamer *trans*-IV), and (iii) normal emission is observed from the rotamer *trans*-IV (mainly) and rotamer *trans*-I in aqueous medium with excitation maximum at 300 nm with shoulder at ~328 nm. The tautomer emission origi-

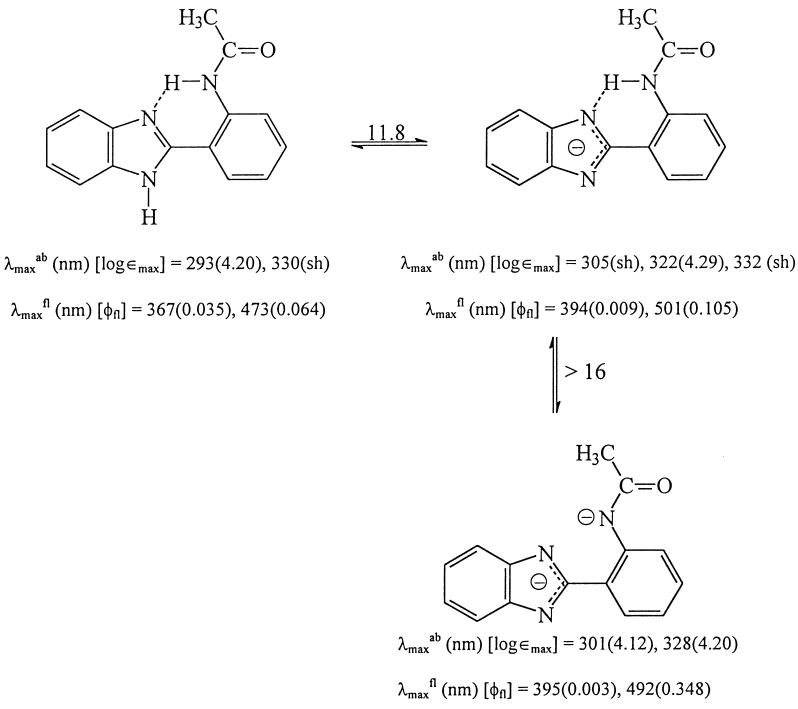


Scheme 2. Absorption band maxima ($\lambda^{ab}_{max}$ nm), molecular extinction coefficient at $\lambda_{max}$ (log $\in_{max}$), fluorescence band maxima ($\lambda^{fl}_{max}$ nm) and fluorescence quantum yields ($\phi_{fl}$) of the normal and tautomer emissions of the neutral monoanion and dianion of 2-AMPBI.

nates from the tautomer *trans*-III, formed by ESIPT in the rotamer *trans*-II (Scheme 1).

As the alkaline concentration increases above pH = 10, the absorption band maximum of the neutral 2-AMPBI shifts towards red and remains unchanged in the pH range of 13–13.5. The band maximum at 318 nm with shoulders at 305 and 332 nm is nicely described by a vibrational frequency of ~1320

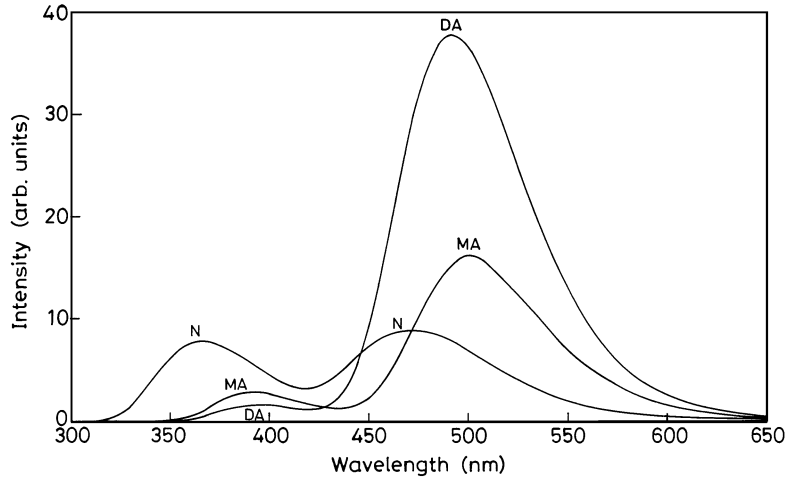


Fig. 1. Fluorescence spectra of 2-AMPBI (1) dianion (DA) $H_-$ = 16; (2) monoanion (MA) $H_-$ = 14; (3) neutral (N) pH = 7. $\lambda_{exc}$ = 290 nm.

$cm^{-1}$. These spectral changes can be assigned to the formation of MAs (Schemes 2 and 3). The observation of an isosbestic point (297 nm) clearly establishes the equilibrium between the neutral-monoanion (N-MA). The $pK_a$ value for the N-MA equilibrium, using absorption data, is found to be 11.8. The

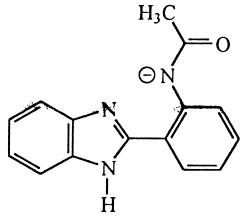

MA-I

$E_{iso}$ = -3026.6873 eV
$E_{sol}$ = -3026.7775 eV
$\mu_g$ = 3.58 D

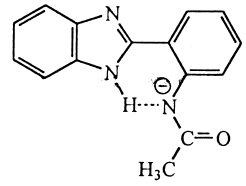

MA-I'

$E_{iso}$ = -3026.7043 eV
$E_{sol}$ = -3026.8061 eV
$\mu_g$ = 3.73 D

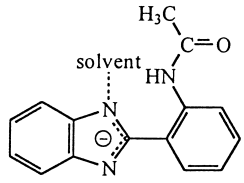

MA-II

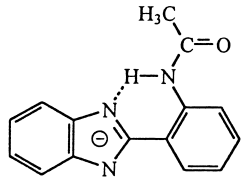

MA-III

$E_{iso}$ = -3026.9709 eV
$E_{sol}$ = -3027.0294 eV
$\mu_g$ = 3.72 D

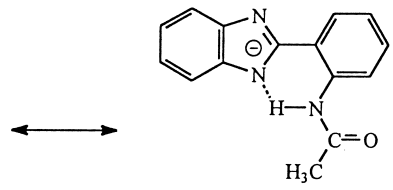

MA-III'

$E_{iso}$ = -3026.9650 eV
$E_{sol}$ = -3026.9794 eV
$\mu_g$ = 3.75 D

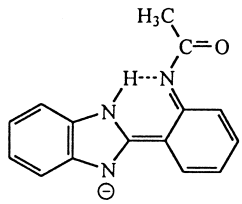

MA-IV

$E_{iso}$ = -3026.8386 eV
$E_{sol}$ = -3027.0887 eV
$\mu_g$ = 5.86 D

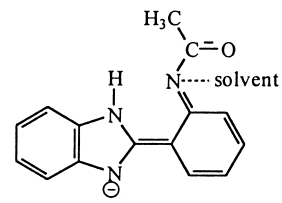

MA-IV'

Scheme 3. Energies of the isolated ($E_{iso}$) and solvated ($E_{sol}$) conformers of MA-I, MA-III and MA-IV of 2-AMPBI and their dipole moment in the ground state ($\mu_g$), obtained using AM1 calculations.

absorption band maxima are given in Scheme 2 and the $pK_a$ value is above the arrows in Scheme 2.

As mentioned earlier, there are two acidic centers in 2-AMPBI and thus MA can be formed by deprotonation of either the >N–H moiety of the benzimidazole (BI, MA-III/MA-III′) ring or of the amide proton (MA-I and MA-I′). Based on earlier data (showing that the $pK_a$ value of the deprotonation of >N–H proton of BI in 2-APBI (12.9) [16] is less than that of the amide proton (> 16 [25]), it can be suggested that MA could be formed only by deprotonation of the >N–H group in the BI moiety (i.e. MA-III/MA-III′). The smaller $pK_a$ value observed for deprotonation of >N–H in 2-AMPBI (11.8) in comparison to that of 2-APBI (12.9) is due to the presence of the electron-withdrawing amide group. The following results further support our above assignment of MA. (i) The results of Scheme 3 show that MA-III and MA-III′ are an energetically similar species as one is the resonance form of the other. This is supported by the vibrational structure ($\bar{\nu}$ = 1330 $cm^{-1}$) observed in the absorption spectrum of MA, which suggests the presence of only one electronic band and thus one species. The vibrational structure in the absorption spectrum is due to the presence of strong intramolecular hydrogen bonding, and (ii) in MA-I′, the ESIPT process is not possible. AM1 calculations have also shown that MA-I and MA-I′ are unstable by ~ 26 kJ $mol^{-1}$ in comparison to MA-III or MA-III′ under isolated conditions and when solvation energy is also included. Furthermore, earlier results have shown [25] that the MA formed by deprotonation of the amide proton is not fluorescent. Further increase in the concentration of NaOH leads to a continuous red shift in the absorption spectrum ($\lambda^{ab}_{max}$ at 328 and 301 nm) and can be assigned to the dianion (DA). Observation of an isosbestic point at 325 nm establishes equilibrium between the monoanion–dianion (MA–DA). Since the formation of DA is not complete even at $H_-$ = 16.5, its $pK_a$ will be greater than 14.8 and is given above the arrows in Scheme 2.

In the pH range of 10.5–12, the fluorescence intensities of both the emission bands of the neutral species decreased without any change in the $\lambda^{fl}_{max}$. At alkaline concentration (pH > 12), dual fluorescence is again observed and both the long (LW, 510 nm) and short (SW, 393 nm) wavelength emissions get red shifted with respect to their corresponding neutral fluorescence bands (473 and 367 nm) and attain maximum intensities at pH ~ 14.5. On further increase of alkaline strength, the fluorescence intensity of the SW emission band starts decreasing without any change in the band shift, whereas that of the LW emission starts increasing with slight blue shift in the fluorescence maximum. This could be due to the formation of DA, which is not complete even at the highest basic concentration. The emission spectra are shown in Fig. 1.

The fluorescence emission spectra of MA ($H_-$ = 14) and DA ($H_-$ = 16) have also been studied using $\lambda_{exc}$ in the range of 310–350 nm. The fluorescence band maxima and the quantum yield remain invariant as a function of $\lambda_{exc}$. This clearly suggests that emissions in both ionic species (MA and DA) are taking place from their most relaxed excited states. The fluorescence excitation spectra of both ionic species were recorded at different emission wavelengths in the range of 370–540 nm. In case of DA, the excitation fluorescence band maxima remain unchanged at different $\lambda_{em}$ of the LW emission bands (not shown) and nearly resemble the absorption spectrum of DA, whereas the fluorescence excitation spectra recorded at SW emission band resemble that of the MA fluorescence excitation spectra, recorded at SW emission. This suggests that not much change is observed in the geometry of DA when excited to the $S_1$ state, whereas the SW emission band of 2-AMPBI at $H_-$ = 16 still belongs to MA and shows, as suggested earlier, that the formation of DA is not complete at $H_-$ = 16. The absence of similar behaviour in the LW emission of DA by MA (still remaining at $H_-$ = 16) could be due to the overlap of the strong emission of DA and not much difference in their respective absorption spectra. On the other hand, the fluorescence excitation band maxima obtained using $\lambda_{em}$ as 370 and 540 nm of MA (Fig. 2) differ slightly (327 and 330 nm) but the tail of the latter excitation spectra is more intense than the former.

Lifetime measurements for both species have also been carried out by exciting at two different wavelenghts (311 and 337 nm) for solutions at $H_-$ = 14 and $H_-$ = 16 and using $\lambda_{em}$ 395, 430, 490 and 540 nm. The lifetimes thus obtained are invariant of $\lambda_{exc}$ and relevant data are compiled in Table 1. The

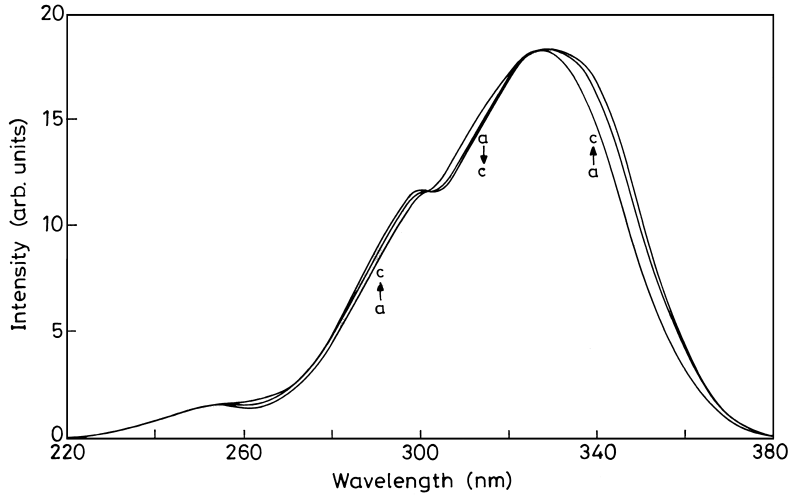


Fig. 2. Fluorescence excitation spectra of monoanion ($H_-$ = 14.0) of 2-AMPBI $\lambda_{em}$ = (a) 370 nm; (b) 440 nm; (c) 540 nm.

fluorescence decay observed at the SW emission of DA followed a biexponential behavior, whereas the fluorescence decay obsserved at the LW emission followed a single exponential behavior. Although the fluorescence decay of the LW emission was also analyzed using biexponential decay, the $\chi^2$ observed in both decay analyses are similar and thus the lifetime observed using a single exponential was used. Furthermore, less than 6% amplitudes of the short-lived species of the biexponential decay proves the above point. In the case of MA, the fluorescence decays at all of the emissions followed a biexponential behavior. The amplitude of the short-lived species decreases and that of the long-lived species increases with an increase in $\lambda_{em}$. Furthermore, the lifetime of the long-lived species of MA is the same at all emission wavelengths, whereas the lifetime of the SW emission ($0.34 \pm 0.02$ ns) is much shorter than that analyzed at the LW emission ($1.0 \pm 0.1$ ns). This suggests that the short-lived ionic species present at the SW emission is different from that observed in the LW emission. Furthermore, lifetimes of

Table 1
Excited-state lifetimes (ns) of neutral, monoanion and dianion of 2-AMPBI measured at different emission wavelengths using single and double exponential analysis

| Species | $\lambda_{cm}$ (nm) | Single exponential | | Double exponential | | | | |
|---|---|---|---|---|---|---|---|---|
| | | $\tau$ | $\chi^2$ | $\tau_1$ | $A_1$ | $\tau_2$ | $A_2$ | $\chi_2$ |
| Dianion ($H_-$ = 16) | 395 | | | 0.32 | 60.8 | 6.03 | 39.2 | 1.22 |
| | 430 | | | 0.34 | 16.9 | 5.92 | 83.1 | 1.18 |
| | 490 | 5.6 | 1.18 | 1.20 | 6.2 | 5.80 | 93.8 | 1.10 |
| | 540 | 5.7 | 1.11 | 1.00 | 3.1 | 5.70 | 96.9 | 1.13 |
| Monoanion ($H_-$ = 14) | 390 | | | 0.33 | 68.5 | 3.70 | 31.5 | 1.28 |
| | 440 | | | 0.36 | 31.9 | 3.90 | 68.1 | 1.24 |
| | 500 | 3.45 | 1.50 | 0.91 | 15.4 | 3.80 | 84.6 | 1.24 |
| | 540 | 3.59 | 1.46 | 1.00 | 16.8 | 3.90 | 83.2 | 1.16 |
| Neutral (pH = 7) | 365 | 0.56 | 1.61 | 0.43 | 86.7 | 6.70 | 13.3 | 1.21 |
| | 420 | | | 0.41 | 48.2 | 6.60 | 51.8 | 1.26 |
| | 480 | 4.74 | 1.14 | 0.81 | 42.2 | 4.70 | 57.8 | 1.25 |
| | 520 | 4.39 | 1.47 | 0.85 | 48.2 | 4.61 | 51.8 | 1.14 |

the short-lived species of the SW and LW emissions at $H_- = 16$ are the same as those observed at $H_- = 14.5$, respectively.

Having established earlier the site of deprotonation in 2-AMPBI, the spectral characteristics of MAs can be explained as follows. The red shifts observed in the absorption and fluorescence spectra of MA in comparison to the neutral species are consistent with the deprotonation of $>$N–H [26,27]. The fluorescence excitation spectra and dual emission suggest the presence of two kinds of MAs, i.e. MA-II (an open structure) and MA-III (a closed structure). The fluorescence excitation maximum at 327 nm and the corresponding lifetime of $0.34 \pm 0.02$ ns can be assigned to MA-II. Whereas the 330 nm fluorescence excitation maximum and the $3.8 \pm 0.1$ ns lifetime can be assigned to the tautomer MA-IV, formed by ESIPT in MA-III. An absence of risetime in tautomer MA-IV (not possible to detect using our instrument) suggests that, similar to the ESIPT process in the neutral species, ESIPT is also very fast in MA-III. Short-lived species in the tautomer emission can be assigned to the solvated structure of the tautomer MA-IV′ as observed in case of the neutral tautomer-III′ and thus can be explained on the same lines [20]. This is supported by the fact that the lifetime of tautomer-IV′ is different from that of MA-II and the amplitude of the short-lived species of tautomer-IV′ remains constant when monitored at 490 or 540 nm. Lastly, the different lifetimes of MA-II and tautomer MA IV and those of MA-IV and MA-IV′ suggest that the equilibrium is not established between these sets of species in the $S_1$ state.

DA can only be formed by deprotonation of the amide proton and thus there can be only one species. This is consistent with the only fluorescence band maximum, similar fluorescence excitation spectra recorded at different $\lambda_{em}$, and single exponential decay observed in the fluorescence decay of the LW emission of DA. The red shift observed in the absorption and fluorescence spectra of DA in comparison to MA is consistent with deprotonation of the amide proton. The small blue shift in the DA emission in comparison to the tautomer emission (MA-IV) is because of the electronic difference between the two ionic species. The presence of the SW emission in DA as stated earlier is due to MA-II, remaining in solution at $H_- = 16$ because of incomplete deprotonation of MA. This is supported by the fact that the fluorescence excitation spectrum of the solution at $H_- = 16$ recorded at the SW emission and the lifetime determined at the SW emission resemble those of MA-II.

$pK_a^*$ values for both equilibria were determined by exciting at the respective isosbetic point and the flourimetric titration curves. The values obtained match the ground-state $pK_a$ values, suggesting that the excited-state equilibria are not established in the $S_1$ state and could be due to the shorter lifetimes of the respective conjugate acid–base pairs. A similar behaviour has also been observed in similar systems [26,27].

## 4. Conclusion

In conclusion, observation of tautomer emission from MA-III suggests that ESIPT can also occur in the monoanion if proper geometrical conditions are satisfied. To our knowledge, this may be the first case.

## Acknowledgements

The authors thank the Department of Science and Technology, New Delhi, for their financial support for Project SP/SI/H-39/96.

## References

[1] A. Douhal, F. Amat-Guerri, A.U. Acuna, J. Phys. Chem. 99 (1995) 76.
[2] A. Douhal, F. Lahmani, A.H. Zewail, Chem. Phys. 207 (1996) 477.
[3] S.J. Formosinho, L.G. Arnuat, J. Photochem. Photobiol. A: Chem. 75 (1993) 21.
[4] D.S. English, W. Zhang, G.A. Kraus, J.W. Petrich, J. Am. Chem. Soc. 118 (1997) 2980.
[5] T. Sekikawa, T. Kobayashi, T. Inabe, J. Phys. Chem. A 101 (1997) 644.
[6] A. Douhal, F. Amat-Guerri, A.U. Acuna, Angew. Chem. Int. Ed. Engl. 36 (1997) 1514.
[7] A. Douhal, Science 276 (1997) 221.
[8] J. Catalan, J.C. Del Valle, J. Am. Chem. Soc. 115 (1993) 4321.

[9] J. Catalan, J.C. Del Valle, R.M. Claramunt, D. Sanz, J. Dotor, J. Luminesc. 68 (1996) 165.
[10] A.U. Khan, M. Khasa, Proc. Natl. Acad. Sci. USA 80 (1983) 1767.
[11] A.U. Acuna, F. Amat-Guerri, J. Catalan, A. Costella, J.M. Figuera, J. Munoj, Chem. Phys. Lett. 132 (1986) 567.
[12] R.W. Munn, Chem. Br. (1989) 517.
[13] F. Vollmer, W. Rettig, J. Photochem. Photobiol. A: Chem. 95 (1996) 143.
[14] A. Sytnik, M. Khasa, Proc. Natl. Acad. Sci. USA 91 (1994) 8627.
[15] B. Dick, N.P. Ernsting, J. Phys. Chem. 91 (1987) 4261, and references listed therein.
[16] A.K. Mishra, S.K. Dogra, J. Photochem. 31 (1985) 333.
[17] H.K. Sinha, S.K. Dogra, Chem. Phys. 102 (1986) 337.
[18] S. Santra, S.K. Dogra, Chem. Phys. 226 (1998) 285.
[19] S. Santra, G. Krishnamoorthy, S.K. Dogra, Chem. Phys. Lett. 311 (1999) 95.
[20] S. Santra, G. Krishnamoorthy, S.K. Dogra, J. Phys. Chem. 104 (2000) 476.
[21] A.R. Tatchell, ELBS, Longman, 1978, pp. 682.
[22] M.J. Jorgenson, D.R. Hartter, J. Am. Chem. Soc. 85 (1963) 878.
[23] M.J.S. Dewar, E.G. Zeoblish, E.F. Healy, J.J.P. Stewart, J. Am. Chem. Soc. 107 (1985) 3092.
[24] J.F. Letard, R. Lepouyard, W. Rettig, Chem. Phys. Lett. 222 (1994) 209.
[25] R. Manoharan, S.K. Dogra, Can. J. Chem. 66 (1988) 2375.
[26] M. Krishnamurthy, P. Phaniraj, S.K. Dogra, J. Chem. Soc. Perkin Trans. II (1986) 1917.
[27] H.K. Sinha, S.K. Dogra, J. Chem. Soc. Perkin Trans. II (1987) 1465.